OTC 6605

The Effect of Wind Spectra on the Low-Frequency Motions of a Moored Tanker in Survival Condition

G.J. Feikema and J.E.W. Wichers, MARIN

ABSTRACT

In the design of moored tankers the knowledge of the wave drift forces is of importance. As is known, the low frequency part of the wave drift forces is responsible for the low frequency motions of the vessel. In general the low frequency motions may cause a substantial part of the mooring forces.

Another source of the low frequency excitation can be found from wind spectra. The wind spectra originate from the turbulence in the wind field. Besides the wave drift forces also the fluctuating wind force will induce low frequency oscillations of the tanker.

The purpose of this study is to investigate the effect of a wind spectrum based on an hourly mean wind speed in relation to the 1-minute steady wind gust, both in combination with a co-linearly directed storm wave spectrum on the low frequency motions of a 200 kDWT tanker.

The tanker is moored in 82.5 m deep water. The computations have been applied to a linear type mooring system. To confirm the reliability of the computation procedure model tests have been carried out.

INTRODUCTION

For the design of a mooring system the environment in terms of storm wave spectrum, current speed and wind velocity has to be established. The irregular waves generate the wave loads, which induce the wave frequency ship motions and the wave drift forces. The wave drift forces consist of a mean wave drift force, a mean wave drift damping and the low frequency wave drift forces. In the design, normally a steady current velocity is taken, while for the wind speed either the steady 3-second, the 1-minute or the 10-minute wind gust speed is taken.

Except for the wave frequency motions, the motions can be distinguished in a mean offset part and a low frequency oscillating part. The mean displacement of the moored vessel is caused by the mean wave drift force, the steady current and wind force. From the point of view of steady offset the mean wave drift force and the steady wind force are often important components in the mooring force.

References and illustrations at end of paper

411

The oscillating part of the wave drift force is responsible for the low frequency oscillating motions of the vessel. In general the low frequency motions may cause a substantial part of the mooring forces.

Another source of the low frequency excitation can be found from wind spectra. The wind spectra originate from the turbulence in the wind field. The description of the turbulence is very complex. However, it is possible to express the turbulence in terms of so-called wind spectra or gust spectra. Studies on wind spectra have been carried out by several researchers as, for instance, Harris [1], DnV [2], Forristal [3], Davenport [4], Ochi-Shin [5] and Wills [6].

Most of the wind spectra contain energy of the wind velocities at the natural periods of the tanker. Because of the relatively light damped system the fluctuating wind velocities generate fluctuating wind forces, which induce low frequency tanker motions.

The effect of the wind spectra on the low frequency motions will be studied. For that purpose a moored tanker has been exposed to the following weather conditions:
- wind spectrum based on an hourly mean wind speed, (V_w = 30.9 m/s)
- storm wave spectrum,
- combination of a steady 1-minute wind gust (V_w = 39.7 m/s) and the storm wave spectrum,
- combination of the wind spectrum based on an hourly wind (V_w = 30.9 m/s) speed and the storm wave spectrum.

By means of computations the low frequency motions have been determined. For the computations the Ochi-Shin and the Harris-DnV wind spectra have been considered. The underlying theory, the computation procedures and the results will be presented.

Model tests have been carried out to check the reliability of the computation procedure. For the validation, however, both in the basin and in the computation the Ochi-Shin spectrum is enhanced by a factor 2π to demonstrate clearly the fluctuating effect of the wind.

For the model tests the wind spectra were generated by wind fans. The wind fans were controlled by means of a microvax computer to generate the wind spectra.

WIND FORCES

Wind forces on moored tankers or offshore structures in general can be split into a number of components:
- A steady component corresponding to some assumed static wind velocity value.
- Dynamic components due to the following effects:
  o turbulence in the undisturbed wind field, which results in time variations of the wind velocity and direction as well as spatial variations;
  o instationary behaviour of the flow around the structure due to vortex shedding and variations in the separation point of the flow.

From the point of view of design and operation of floating offshore structures the steady component is important but also attention should be paid to the instationary part of the wind force.

Static wind force

The equations for the static component of the wind forces on tankers are as follows:

$$X_{1w} = \tfrac{1}{2}\rho \, C_{1w}(\psi_w) \, A_t \, V_w^2$$

$$X_{2w} = \tfrac{1}{2}\rho \, C_{2w}(\psi_w) \, A_1 \, V_w^2$$

$$X_{6w} = \tfrac{1}{2}\rho \, C_{6w}(\psi_w) \, A_1 \, L \, V_w^2$$

in which:
ρ = specific density of air
C_{1w} = resistance coefficient in surge direction
C_{2w} = resistance coefficient in sway direction
C_{6w} = resistance coefficient in yaw direction
ψ_w = wind angle
A_t = frontal wind area
A_1 = lateral wind area
V_w = wind velocity
L = length between perpendiculars
1,2,6 = surge, sway and yaw mode of motion

412

The wind forces on offshore structures are generally determined from model tests in wind tunnels. A model of the structure is fixed to a force balance by means of which the three forces and the three moments acting on the structure can be measured. In measuring the wind forces on a floating structure, a flat plate is usually situated at the level of the waterline of the vessel, thus ensuring that only the above-water part of the structure is exposed to the wind. The wind force coefficients for tankers determined by means of wind tunnel tests are given by OCIMF, ref. [7].

Not only the wind velocity but also the vertical wind velocity distribution is of importance. The vertical wind velocity profile expresses the reduction of the wind velocity closer to the sea surface due to friction effects.

The following relation is often used:

$$V_w(z) = V_w(10)(z/10)^{1/7}$$

in which:
z = vertical distance above the mean sea level in m
$V_w(10)$ = reference wind speed measured 10 m above sea level.

In high seas the wind velocity near the water surface is influenced by the wave profile. This is usually not taken into account in wind tunnel testing, but has been investigated in some cases. In this case the flat plate has been replaced by a rigid wavy surface. The influence of applying a wavy surface instead of a flat surface on the vertical wind velocity profile is shown in Fig. 1. It must be noted that in reality the wavy surface is not fixed in space but is travelling with the wind velocity.

Dynamic effects in wind velocity

For the computation of the wind forces on a structure a mean wind speed in combination with the turbulence in the wind field should be taken into account. A measure for the wind turbulence relates the mean wind velocity and the variation about the mean wind velocity:

$$\tau_w = \sigma/V_w$$

in which:
σ = rms value of the measured wind velocity
V_w = the reference mean wind velocity.

The description of the turbulence is very complex. However, several investigators have tried to express the turbulence in terms of a so-called wind spectrum or gust spectrum, most of them derived from prototype measurements.

Some of the formulations are summarized below:

Harris-Det norske Veritas (refs. [1], [2], [3]):

$$f\, S_{V_w}(f) = 4\, C\, V_w^2\, F_g$$

$$F_g = x/(2 + x^2)^{5/6}$$

$$x = 1800\; f/V_w$$

or:

$$S_{V_w}(\omega) = \frac{7200}{2\pi}\, C\, V_w/\left[2 + (286\, \omega/V_w)^2\right]^{5/6}$$

where:
F_g = gust factor
C = turbulence or surface drag coefficient; may be chosen equal to 0.002 for "rough" seas and 0.0015 for "moderate" seas
V_w = the hourly mean wind speed (m/s) at a reference level 10 m above the water surface
L = length scale dimension (m); may be chosen equal to 1800 m
f = frequency of the wind oscillations in Hz
ω = frequency of the wind oscillations in rad/s
S_{V_w} = spectral density of the wind velocity in m^2/s

Fig. 2 shows a typical spectrum of wind speed during Hurricane Eloise from data measured at an oil platform in EI331 (Northern Gulf of Mexico; September 22-23, 1975). The reference wind speed amounts to 17.73 m/s. The wind spectrum is compared with the Harris-DnV spectrum formulation. For the surface drag coefficient 0.002 was used.

<u>Davenport (ref. [4])</u>:

$$f\ S_{V_w}(f) = 4\ C\ V_w^2\ F_g$$

$$F_g = x^2/(1 + x^2)^{4/3}$$

$$x = 1200\ f/V_w$$

or:

$$S_{V_w}(\omega) = \left(\frac{916700}{2\pi}\right)\ C\ \omega/\left[1 + (191\ \omega/V_w)^2\right]^{4/3}$$

The formulation of Davenport originates from measurements on land. Comparing this formule with other ones it can be found that the low frequency energy has vanished. The absence of the energy is probably caused by the dissipation due to the presence of the relatively high obstacles on land.

<u>Ochi-Shin (ref. [5])</u>:

$$f\ S_{V_w}(f) = C\ V_w^2\ F_g$$

in which the gust factor F_g is defined as follows:

$0 \leq f \leq 0.0003\ V_w$ $\quad$ $F_g = 583\ x$

$0.0003\ V_w \leq f$
$f \leq 0.01\ V_w$ $\quad$ $F_g = \dfrac{420\ x^{0.7}}{(1 + x^{0.35})^{11.5}}$

$f \geq 0.01\ V_w$ $\quad$ $F_g = \dfrac{838\ x}{(1 + x^{0.35})^{11.5}}$

where:
$x = z\ f/V_w(z)$
z = height above sea level (10 m);

or in rad/s:

$$\omega\ S_{V_w}(\omega) = C\ V_w^2\ F_g$$

in which the gust factor F_g is defined as follows:

$0 \leq \omega \leq 0.001885\ V_w$ $\quad$ $F_g = 583\ x$

$0.001885\ V_w \leq \omega$
$\omega \leq 0.0628\ V_w$ $\quad$ $F_g = \dfrac{420\ x^{0.7}}{(1 + x^{0.35})^{11.5}}$

$f \geq 0.0628\ V_w$ $\quad$ $F_g = \dfrac{838\ x}{(1 + x^{0.35})^{11.5}}$

where:
$x = 1.592\ \omega/V_w$

V_w = mean wind speed at a reference level of 10 m.

In the formulation of the surface drag coefficient C, the results of Wu as shown in Fig. 3 have been used by Ochi and Shin. In formula form the drag coefficient is given below:

$$C = (750 + 69\ V_w) * 10^{-6}$$

<u>Modified Harris spectrum or Wills spectrum (Ref. [6])</u>:

$$f\ S_{V_w}(f) = 4\ C\ V_w^2\ Fg$$

$$F_g = x\ A(x)/(2 + x^2)^{5/6}$$

$$x = 1800\ f/V_w$$

$$A(x) = 0.51\left[(2+x^2)^{5/6}/(x^{0.15} + \tfrac{9}{8}\ x)^{5/3}\right]$$

$$C = \text{roughness parameter} = 0.003$$

or:

$$S_{V_w}(\omega) = \left(\frac{3672}{2\pi}\ C\ V_w\right)/\left(x^{0.15} + \tfrac{9}{8}\ x\right)^{5/3}$$

where $x = 286.5\ \omega/V_w$.

For reason of comparison the results of the above mentioned formulations based on an hourly mean wind velocity of 30.9 m/s at 10 m above sea level are given in Fig. 4.

VERTICAL WIND PROFILE AND STEADY GUST WIND VELOCITY

As mentioned before the vertical wind velocity profile expresses the reduction of the wind velocity closer to the sea surface due to friction effects. Formulae exist to describe the vertical wind profiles. In many design problems it is useful to know the maximum wind speed averaged over some short time interval. From literature the relations between steady gust wind velocities over average time intervals can be found. A review of some of the formulae is given below.

Bretschneider (ref. [8]):

The relationship often chosen for the vertical profile using the boundary layer profile for the wind is given by ref. [8]:

$$V_w(z) = V_w(10)(z/10)^{1/7}$$

in which:

$V_w(10)$ = average wind velocity 10 m above sea surface

$V_w(z)$ = wind velocity z m above the sea surface.

The periods over which the average value is determined may vary from 3 seconds to 60 minutes. The 3-second mean wind speed is called the 3-second gust. Contrary to the application of wind spectra the (sustained) wind speed averaged over, for instance, 3 seconds or 1 minute is often used for the design. This ensures in most cases that the complete structure has been subjected to the same wind field. When no specific data are available for the sustained wind speed averaged over a short period, this speed can be approximated from the wind speed averaged over a different period using the following empirical relationship:

$$V_w(t2) = V_w(t1)[1 + 0.16 \log (t1/t2)]$$

in which:

$V_w(t2)$ = wind speed averaged over t2
$V_w(t1)$ = wind speed averaged over t1

DnV (ref. [2]):

In absence of more reliable data, the wind speed as a function of height above the mean water level and averaging time interval may be approximated by the following power law:

$$V_w(t,z) = \alpha V_w (z/10)^{\beta}$$

in which:

$V_w(t,z)$ = the wind speed averaged over a time interval t as defined by α and β, z metres above the mean water level

V_w = the wind speed averaged over one hour, 10 m above sea level

α = gust factor referenced to V_w
β = height exponent.

The factors in the power law for the wind profiles are shown in the table below:

Factor	Average time interval					
	1 hr	10 min	1 min	15 s	5 s	3 s
α	1.000	1.060	1.180	1.260	1.310	1.330
β	0.150	0.130	0.113	0.106	0.102	0.100

Ochi-Shin (ref. [5]):

The formula for the vertical wind profile as used by Ochi and Shin reads as follows:

$$V_w(z) = V_w + 2.5 \sqrt{C} \, V_w \, \ln(z/10)$$

in which C = the drag surface coefficient.

Modified Harris or Wills spectrum (ref. [7]):

For the modified Harris wind spectrum the wind speeds are described by the 10 minute average wind speed given at 10 m above the sea level. The wind speeds for other averaging periods (t) and at other heights (z) above the sea level may be computed as follows:

$$V_w(t,z) = V_w(600,z) \, [1 + 0.137 \ln(z/10) + \\ - 0.047 \ln(t/600)]$$

Wind force spectrum

In order to compute the effect of the oscillating wind velocities on the moored tanker, time domain computations have been carried out. For the computations not only the description of the wind spectrum but also the statistical distribution of the wind velocity has to be known. Based on the results in ref. [9] it can be assumed that the turbulence is Gaussian. An example of the Gaussian distribution of the oscillating wind as derived from ref. [9] is shown in Fig. 5. Given the shape of the wind spectrum the oscillating wind speed can be approached as a time series by means of a finite summation technique (or random noise theory):

$$V_w(t) = \sum_{j=1}^{N} \left[\sqrt{2S_{V_w}(\omega_j)\Delta\omega} \cos\{\omega_j t + Q(j)\} \right] + V_w$$

in which:

N = number of spectral values

$S_{V_w}(\omega_j)$ = array with spectral values

$\Delta\omega$ = delta-frequency of spectrum in rad/s

t = time

$Q(j)$ = random variable, uniformly distributed in the interval $[0, 2\pi]$

V_w = mean wind velocity at a reference level of 10 m.

Having the time domain trace of the wind velocity, the wind force trace on a surface can be computed if the wind resistance coefficient is known. Spectral analysis of the wind force trace may deliver the wind force spectrum.

A straight derivation of the wind spectrum into a wind force spectrum by knowing the wind area, for instance the frontal area of a tanker A_t and the associated wind resistance coefficient $C_{1w}(180°)$, can be obtained. For the derivation it is assumed that the mean wind velocity (for instance the hourly mean wind speed V_w) is always larger than the oscillating wind components $V(t)$.

The total wind force acting on the fixed tanker will be:

$$X_{1w}(t) = \tfrac{1}{2}\rho\, C_{1w}(180°)\, A_t\, (V_w(t))^2$$
$$= \tfrac{1}{2}\rho\, C_{1w}(180°)\, A_t\, (V_w + V(t))^2$$
$$= \tfrac{1}{2}\rho\, C_{1w}(180°)\, A_t\, V_w^2 +$$
$$(2\,\tfrac{1}{2}\rho\, C_{1w}(180°)\, A_t\, V_w^2 /V_w)\, V(t) +$$
$$\tfrac{1}{2}\rho\, C_{1w}(180°)\, A_t\, (V(t))^2$$
$$= X_{1w}^{(1)} + (2X_{1w}^{(1)}/V_w)\, V(t) +$$
$$(X_{1w}^{(1)}/V_w^2)\, (V(t))^2$$

The first term represents the mean wind force on the tanker. The second term is an oscillating wind force with frequencies corresponding to the frequencies of the wind spectrum with an average of zero. The last term, however, is of quadratic nature. Such a term contains not only a mean part, but also oscillating parts in the $(\omega_i - \omega_j)$ and $(\omega_i + \omega_j)$ frequency range.

Neglecting the parts with the sum frequencies an analogy with the wave drift forces can be made. For reason of analogy it may be assumed that the oscillating wind $V(t)$ can be replaced by the wave height $\zeta(t)$.

In terms of spectral density of the wind forces the second term can be read as follows:

$$S_{X_{1w}^{(1)}}(\omega)\,\Delta\omega = \tfrac{1}{2}(X_{1w}(\omega))^2$$
$$= \tfrac{1}{2}((2X_{1w}^{(1)}/V_w)\, V(\omega))^2$$
$$= (2X_{1w}^{(1)}/V_w)^2\, S_V(\omega)\,\Delta\omega$$

or:

$$S_{X_{1w}^{(1)}}(\omega) = (2X_{1w}^{(1)}/V_w)^2\, S_V(\omega)$$

For the third term the spectral density of the wind force can be derived as follows:

$$(V(t))^2 = \sum_{i=1}^{N}\sum_{j=1}^{N} V_{ai}\, V_{aj}\, \sin(\omega_i t + \varepsilon_i) * $$
$$\sin(\omega_j t + \varepsilon_j)$$

while the low frequency part will read:

$$(V_1(t))^2 = \tfrac{1}{2}\sum_{i=1}^{N}\sum_{j=1}^{N} V_{ai} V_{aj}[\cos\{(\omega_i - \omega_j)t + (\varepsilon_i - \varepsilon_j)\}]$$

in which the mean part of the quadratic wind velocity $V(t)$ amounts to:

$$(\bar{V})^2 = \tfrac{1}{2}\sum_{n=1}^{N} (V_{an})^2$$
$$= \int_0^{\infty} S_V(\omega)\, d\omega = m_0$$

in which m_0 = area of the spectrum of the wind velocity, and the corresponding mean wind force amounts to:

$$X_{1w}^{(2)} = m_0(X_{1w}^{(1)}/V_w^2)$$

while the low frequency oscillating part can be read as follows:

$$S_{X_{1w}^{(2)}}(\mu) = 8 \int_0^\infty S_V(\omega) \cdot S_V(\omega+\mu)(X_{1w}^{(1)}/V_w)^2 d\omega$$

in which $\mu = \omega_i - \omega_j$

The total spectral density of the wind force at the natural frequency μ_e of the moored tanker will be:

$$S_{X_{1w}}(\mu_e) = (2X_{1w}/V_w)^2 S_V(\mu_e) +$$
$$8 \int_0^\infty S_V(\omega) \; S_V(\omega+\mu_e)(X_{1w}^{(1)}/V_w^2)^2 d\omega$$

while the total mean wind force amounts to:

$$X_{1w}(\text{total}) = X_{1w}^{(1)} + m_0 \; (X_{1w}^{(1)}/V_w^2)$$

Computations

Computations have been carried out on the low frequency motions of a moored 200 kDWT tanker in 82.5 m water depth. The particulars of the tanker are given in Table 1, while the body plan is shown in Fig. 6. The tanker is exposed to co-linearly directed waves and wind. The tanker was moored in linear springs with a spring constant in surge direction $C_{11} = 13.9$ tf/m. The set-up of the mooring system is given in Fig. 7.

The tanker has been exposed to following weather conditions:

1. Wave spectrum $H_s = 9.47$ m; $T_1 = 11.55$ s

   Ochi-Shin wind spectrum:
2. Ochi-Shin wind spectrum $V_w(1 \text{ hr}) = 30.9$ m/s
3. Wave spectrum $H_s = 9.47$ m; $T_1 = 11.55$ s + Ochi-Shin wind spectrum V_w (1 hr) = 30.9 m/s
   1-minute-gust (Bretschneider):
4. Wave spectrum $H_s = 9.47$ m; $T_1 = 11.55$ s + 1 minute gust wind (Bretschneider: V_w (1 min) = 39.7 m/s)

   Harris-DnV wind spectrum:
5. Harris-DnV wind spectrum V_w (1hr) = 30.9 m/s
6. Wave spectrum $H_s = 9.47$ m; $T_1 = 11.55$ s + Harris-DnV wind spectrum V_w (1 hr) = 30.9 m/s

1-minute gust DnV:
7. Wave spectrum $H_s = 9.47$ m; $T_1 = 11.55$ s + 1 minute gust wind (DnV): V_w (1 min) = 36.5 m/s

For the weather conditions 1-7, frequency domain computations were carried out for both the loaded and ballasted tanker.

The applied wave spectrum and the associated wave group spectrum are given in the Figs. 8 and 9. The theoretical wind spectra are shown in Fig. 4.

Frequency domain computations

For the frequency domain the mean displacement, the standard deviation and the most probable maximum excursion for a storm duration of 3 hours are determined according to the theory as given in refs. [10], [14]:

- the mean displacement can be read as follows:

$$\bar{x}_1 = (X_{1w}^{(1)} + X_{1w}^{(2)} + X_1^{(2)})/C_{11}$$

- the natural frequency will be:

$$\mu = \sqrt{C_{11}/(m + a_{11})}$$

- the variance of the low frequency surge motion can be expressed as follows:

$$(\sigma_{x_1})^2 = \pi \left[S_{X_1^{(2)}}(\mu_e) + S_{X_{1w}}(\mu_e) \right] / \left[2 \; (b_{11} + b_{1w} + b_{1m} + B_{11}) \; C_{11} \right]$$

- while the most probable maximum surge motion in a time period T will be:

$$x_{max} \approx \bar{x}_1 + \sigma_{x_1} \sqrt{2 \ln N}$$

in which:

$\bar{x}_1$ = mean displacement

$X_1^{(2)}$ = mean wave drift force

$X_{1w}^{(1)}$ = mean wind force, first order contribution

417

$X_{1w}^{(2)}$ $= m_0(X_{1w}^{(2)}/V_m^2)$

= mean part of oscillating wind force

C_{11} = spring constant in surge direction

μ_e = natural frequency of system

m = mass of the tanker

a_{11} = added mass at the natural frequency of the system

σ_{x_1} = standard deviation of the low frequency surge motion

$S_{X_1}^{(2)}(\mu_e)$ = spectral density of wave drift force at the natural frequency of the system

$S_{X_{1w}^{(1)}}(\mu_e)$ = spectral density of wind force at the natural frequency of the system in surge direction

$S_{X_{1w}^{(2)}}(\mu_e)$ = second order contribution to the spectral density of the wind force at the natural frequency of the system in surge direction

$b_{11}(\mu_e)$ = viscous damping at the natural period in surge direction

b_{1w} = $2X_{1w}^{(1)}/V_w$ = wind damping

b_{1m} = damping due to mooring system

B_{11} = wave drift damping

x_{max} = most probable maximum excursion during N oscillations

N = number of low frequency oscillations in the considered storm time period.

The input data and the results are presented in Tables 2 through 5. For the calculation of $S_{X^{(2)}}(\mu_e)$ and $X_{1w}^{(2)}$ the wind spectrum was cut off at 0.157 rad/s. This corresponds to the Nyquist criterion for a sample time of 20 s. The computed spectral densities of wave drift forces for both the loaded and ballasted tanker are given in Fig. 10. The applied quadratic transfer function of the wave drift forces and the wave drift damping are given in the Figs. 11 and 12.

VALIDATION

Model tests

In order to validate the computation procedure a series of model tests were carried out with a fully loaded 200 kDWT tanker. The applied scale was 82.5. All model data were scaled to full scale according to Froude's law of similitude.

The model tests were carried out in the Shallow Water Basin, which measures 220 * 16 * 1.1 m in length, width and maximum water depth respectively. Water depth is adjustable. The basin is equipped with wave makers on one short side. A beach at the opposite side absorbs the incoming waves. Prior to the tests a wave spectrum was adjusted with H_s = 9.47 m and T_1 = 11.55 s. The waves were measured at the projected location of the COG of the tanker. The generated wave spectrum, the distribution of the wave elevation and the wave group spectrum are shown in Figs. 8 and 9.

In the tank a battery of wind fans was positioned in front of the tanker. The wind fans produced a relatively homogeneous wind field, which was wide enough to cover the test set-up of the tanker and a wind gauge. These wind fans were connected to a control system which enabled the control of the RPM of the fans. This control system was connected to a microcomputer. By the side of the tanker a wind gauge was placed. The output signal of this gauge was input to the microcomputer. Through a control algorithm the measured wind speed was used to generate an input signal to the control system of the fans. In this algorithm the above described theoretical wind spectra were programmed. This system of wind gauge, microcomputer, control algorithm and wind fan control was able to generate a typical wind spectrum. Prior to the tests the 2π-enhanced Ochi-Shin wind spectrum corresponding to an 1 hour mean wind speed of 30.9 m/s was adjusted. The adjusted spectrum is shown in Fig. 15.

The tanker was moored in a system of springs giving a total stiffness for the

surge motion of 13.9 tf/m. The surge motion was measured in the COG by means of an optical tracking device. On top of the tanker a deckhouse was mounted with a projected front area of 1,000 m^2. The test set-up is shown in Fig. 7. A surge decay test was carried out to determine the natural frequency and the viscous damping $b_{11}(\mu)$.

The test duration of each of the applied weather conditions 1 through 4 amounted to 6 hours for full scale. The measured surge motions were subjected to low-pass filtering. To the low frequency surge motion statistical analyses were applied. Further, the low frequency peak values in backward surge direction with regard to zero (equilibrium position) were plotted on Weibull paper in order to determine the most probable surge motion (P(most probable maximum)=1/N*100%), which can occur during a storm of 3 hours with N low frequency oscillations. The results of the analysis are given in Table 6.

The results of the model tests have been correlated with the results of both frequency and time domain simulations.

Time-domain computations

In the time domain the following equation of motion has to be solved:

$$(m+a_{11})\ddot{x}_1+(b_{11}+B_{11})\dot{x}_1+C_{11}x_1$$
$$= X_{1w}(\dot{x}_1,t) + X_1^{(2)}(t)$$

in which:

$$X_{1w}(\dot{x}_1,t) = \tfrac{1}{2}\rho\, C_{1w}(180°)\, A_t\, (V_w(t)+\dot{x}_1)^2$$

and

$$V_w(t) = \sum_{j=1}^{N} \left[\sqrt{2\, S_{V_w}(\omega_j).\Delta\omega}\, \cos\{\omega_j t + Q(j)\} \right] + V_w$$

From the time trace of the computed wind velocity the spectrum has been determined. The result is given in Fig. 13. From Fig. 4 it can be concluded that the generated spectrum corresponds rather well with the theoretical one.

To generate the wave drift force $X_1^{(2)}(t)$ use is made of a simplified model as is extensively described in refs. [13] and [14]. The model is based on a bandwidth limited white noise representation of the low frequency force components with an exponential distribution.

The spectral density of the simplified excitation force is equal to the spectral density of the "true" wave drift force for the natural frequency of the system. In terms of mathematical expressions the aforementioned description for the wave drift force will be:

$$X_1^{(2)}(t) = \sigma_{X_1^{(2)}}(A+1) + X_1^{(2)}$$

in which:
A = ln(rnd(a)) for 0 < rnd(a) $\leq$ 1.

The quantity A represents an exponential distribution with average of minus one while the standard deviation amounts to one. For the white noise representation the total energy of the wave drift force is found from:

$$m_0 = S_{X_1^{(2)}}(\mu_e)\, \pi/\Delta t$$

in which:
$\pi/\Delta t$ = Nyquist frequency being the maximum observed frequency.

The variance of the wave drift force $X_1^{(2)}(t)$ will be:

$$(\sigma_{X_1^{(2)}})^2 = E[(X_1^{(2)}(t))2] - \{E[(X_1^{(2)}(t)]\}^2$$

or

$$(\sigma_{X_1^{(2)}})^2 = S_{X_1^{(2)}}(\mu_e)\, \pi/\Delta t$$

Taking a sample frequency of once every Δt the function $X_1^{(2)}(t)$ can be computed. In Fig. 14 an example is given of the distribution of the low frequency surge force on a large tanker in irregular head waves. In this case it concerns measurements carried out by MARIN. In the same figure a line is drawn showing the exponential distribution assumed in the simplified excitation model. As can be seen the agreement is reasonable.

As mentioned before, model tests and time domain computations were carried out to validate the frequency domain computations. Because the frequency-domain computations actually stand for a realization with a duration of infinity, for the time domain computations long duration runs of 60 hours were performed in order to have sufficient statistical low frequency data.

To the low frequency (time domain) surge motions statistical analyses were applied. Further, the low frequency peak values in backward surge direction with regard to zero (equilibrium position) were plotted on Weibull paper in order to determine the most probable surge motion (P(most probable maximum) = 1/N*100%) for a storm duration of 3 hours.

The validated results of the model tests and the computations are presented in Table 6. Comparing the results it can be concluded that a rather good agreement was found.

DISCUSSION OF RESULTS

- The simulation of large scale turbulence in the wind field resulting in a fluctuating wind speed is possible in the model basin. The distribution of energy over the different frequencies can be controlled, enabling the generation of different theoretical wind spectra.

- The computation procedures have been validated by means of model tests. The results of the models agree rather well with the results of both the time domain and frequency domain computations. Deviations in results may be caused by the limited statistical convergence of a realization of 6 hours full scale of the model tests.

- For the computations the loaded and the ballasted tanker were exposed to both wind spectra and to an 1-minute gust, all in combination with a storm wave spectrum.

- The effect of the Ochi-Shin spectrum was compared with the Bretschneider 1-minute gust and the Harris-DnV wind spectrum with the DnV 1-minute gust. Considering the most probable maximum in a 3-hour storm it can be concluded that in all

cases the steady 1-minute wind gust gives higher low frequency surge motions, although the oscillation motions in a combined wave/wind spectrum are larger than in the combined wave spectrum/1-minute gust. The mean wind force caused by the 1-minute gust is mainly responsible for the larger most probable maximum.

- In literature a large number of formulations for wind spectra are known with relatively large differences, especially in the low frequency range, see Fig. 4. The selection of the wind spectra must be done carefully since it may influence the design. The Davenport spectrum, which actually applies to land-built structures and contains hardly low frequency oscillating wind velocities, is not of interest for floating structures at sea.

- Starting from an one hourly wind velocity of 30.9 m/s, different formulations produce different values for the wind gust velocity. This is shown in the following table:

Formulation	Wind gust velocities (m/s)			
	1 hr	10 min	1 min	3 s
DnV	30.9	32.8	36.5	41.1
Wills	30.9	33.7	37.3	42.1
Bretschneider	30.9	34.7	39.7	46.1

The wind gust interval and the appropriate formulation of the velocity must be chosen carefully since it may influence the design of the mooring forces.

CONCLUSIONS

- There is a large number of formulations for wind spectra and gust factors known in literature. Especially in the low frequency range the wind spectra show large differences.

- It has been shown that generation of wind spectra in the tank is feasible. The results of the model tests with a moored tanker show good correlation with

the frequency and time domain simulations.

- For both the fully loaded and ballasted tanker the most probable low frequency surge motions are larger for the storm wave spectrum/1-minute gust than for the corresponding storm wave/wind spectrum.

REFERENCES

1. Harris, R.I.: "The Nature of the Wind, the Modern Design of Wind Sensitive Structures", Const. Ind. Res. & Inf. Assn., London, 1971, pp. 29-55.

2. Det norske Veritas: "Rules for the Design-Construction and Inspection of Offshore Structures", 1977, Appendix A/Environmental Conditions (reprint with corrections 1982).

3. Forristal, G.Z.: "Wind Spectra and Gust Factors over Water", OTC paper 5735, Houston, 1988.

4. Davenport, A.G.: "The Spectrum of Horizontal Gustiness near the Ground of High Winds", Quarterly Journal Royal Meteorological Society, Vol. 87, 1961, pp. 194-211.

5. Ochi, M.K. and Shin, Y.S.: "Wind Turbulent Spectra for the Design Consideration of Offshore Structures", OTC paper 5736, Houston, 1988.

6. Wills, J.A.B.: "Analysis of High-Wind Spectra from the NMI West Sole Experiment for Shell", NMI project No. 3511534, 7 volumes.

7. OCIMF: "Prediction of Wind and Current Loads on VLCC's", OCIMF, 6th Floor, Portland House, Stag Place, London, 1977.

8. Bretschneider, C.L.: "Wave and Wind Loads" Section 12 of Handbook of Ocean and Underwater Engineering, McGraw-Hill Book Company, New York, 1969.

9. Shinju Kato, Sadao Ando, Hiroshi Sato and Yutaro Motora: "At-Sea Experiment of a Floating Offshore Structure, Part 1 Wind Characteristics at the Test Field", Journal of The Society of Naval Architects of Japan, Vol. 167, June 1990.

10. Wichers, J.E.W.: "On the Low Frequency Surge Motions of Vessels Moored in High Seas", OTC paper 4437, Houston, 1982.

11. Wichers, J.E.W.: "A Simulation Model for a Single Point Moored Tanker", Doctoral Thesis, Delft University of Technology, 1988.

12. Pinkster, J.A. and J.E.W. Wichers: "The Statistical Properties of Low-Frequency Motions of Non-Linearly Moored Tankers", OTC paper 5457, Houston, 1987.

13. Pinkster, J.A.: "On the Determination of the Statistical Properties of the Behaviour of Moored Tankers", Proceedings of a Workshop on Floating Structures and Offshore Operations, Wageningen, The Netherlands, Nov. 1987.

Table 1 - Particulars of 200 kDWT tanker

Designation	Symbol	Unit	Magnitude 100% T	Magnitude 40% T
Length between perpendiculars	L_{pp}	m	310.00	310.00
Breadth	B	m	47.17	47.17
Depth	D	m	29.70	29.70
Draft	T	m	18.90	7.56
Displacement weight	Δ	tf	240,869	91,180
Centre of gravity above keel	KG	m	13.32	13.32
Centre of buoyancy forward of section 10	FB	m	6.60	10.46
Metacentric height	GM	m	5.78	13.94
Longitudinal radius of gyration in air	k_{yy}	m	77.47	82.15
Natural pitch period	T_ϕ	s	10.80	–
Waterplane coefficient	C_W	–	0.90	–
Midship section coefficient	C_M	–	0.95	–
Block coefficient	C_B	–	0.85	–
Frontal wind area (superstructure)	FW	m²	1000	1000

Table 2 - Input data and results of the frequency-domain computations

Loaded tanker/Ochi-Shin wind spectrum

Data		Wind spectrum V_w = 30.9 m/s	Wave spectrum	1-minute gust V_w = 39.7 m/s Wave spectrum	Wind spectrum V_w = 39.7 m/s Wave spectrum	Wind spectrum V_w = 30.9 m/s Wave spectrum
INPUT DATA FOR FREQUENCY DOMAIN:						
a_{11}	[tf.s².m]	1594.0	1594.0	1594.0	1594.0	1594.0
m	[tf.s².m]	24553.0	24553.0	24553.0	24553.0	24553.0
b_{11}	[tf.s.m⁻¹]	17.9	17.9	17.9	17.9	17.9
b_{1v}	[tf.s.m⁻¹]	5.8	0.0	7.5	7.5	5.8
B_{11}	[tf.s.m⁻¹]	0.0	34.3	34.3	34.3	34.3
b(tot)		23.7	52.2	59.7	59.7	58.0
c_{11}	[tf.m⁻¹]	13.9	13.9	13.9	13.9	13.9
$x_1^{(2)}$	[tf]	0.0	-115.4	-115.4	-115.4	-115.4
$x_{1v}^{(1)}$	[tf]	-89.6	0.0	-147.9	-147.9	-89.6
$x_{1v}^{(2)}$	[tf]	-0.9	0.0	0.0	0.0	-0.9
X_1(tot)		-90.5	-115.4	-263.3	-263.3	-205.9
$S_{x_1}^{(2)}$	[tf².s]	0.0	79212.0	79212.0	79212.0	79212.0
$S_{x_1}^{(1)}$	[tf².s]	2778.0	0.0	0.0	0.0	2778.0
$S_{x_{1v}}^{(2)}$	[tf².s]	39.0	0.0	0.0	0.0	39.0
S_{X_1}(tot)		2817.0	79212.0	79212.0	79212.0	82029.0
FREQUENCY DOMAIN						
$\bar{x}_1$	[m]	-6.5	-8.3	-18.9	-18.9	-14.8
σ_{x_1}	[m]	3.7	13.1	12.2	12.2	12.6
T	[s]	272.0	272.0	272.0	272.0	272.0
N (3 hrs)	[-]	39.7	39.7	39.7	39.7	39.7
x_{max} (3 hrs)	[m]	-16.5	-43.8	-52.2	-52.2	-49.1

Table 3 - Input data and results of the frequency-domain computations

Ballasted tanker/Ochi-Shin wind spectrum

Data		Wind spectrum V_w = 30.9 m/s	Wave spectrum	1-minute gust V_w = 39.7 m/s Wave spectrum	Wind spectrum V_w = 30.9 m/s Wave spectrum
INPUT DATA FOR FREQUENCY DOMAIN:					
a_{11}	[tf.s^2.m]	250.0	250.0	250.0	250.0
m	[tf.s^2.m]	9295.0	9295.0	9295.0	9295.0
b_{11}	[tf.s.m^{-1}]	16.0	16.0	16.0	16.0
b_{1v}	[tf.s.m^{-1}]	7.2	0.0	9.2	7.2
B_{11}	[tf.s.m^{-1}]	0.0	10.7	10.7	10.7
b(tot)		23.2	26.7	35.9	33.9
c_{11}	[tf.m^{-1}]	13.9	13.9	13.9	13.9
$x_1^{(2)}$	[tf]	0.0	-88.9	-88.9	-88.9
$x_{1v}^{(1)}$	[tf]	-110.4	0.0	-182.2	-110.4
$x_{1v}^{(2)}$	[tf]	-1.1	0.0	0.0	-1.1
X_1(tot)		-111.5	-88.9	-271.1	-200.4
$S_{x_1^{(2)}}$	[tf^2.s]	0.0	43260.0	43260.0	43260.0
$S_{x_{1v}^{(1)}}$	[tf^2.s]	4218.0	0.0	0.0	4218.0
$S_{x_{1v}^{(2)}}$	[tf^2.s]	52.0	0.0	0.0	52.0
S_{X_1}(tot)		4270.0	43260.0	43260.0	47530.0
FREQUENCY DOMAIN					
$\bar{x}_1$	[m]	-8.0	-6.4	-19.5	-14.4
σ_{x_1}	[m]	4.6	13.5	11.7	12.6
T_1	[s]	165.0	165.0	165.0	165.0
N (3 hrs)	[-]	65.5	65.5	65.5	65.5
x_{max} (3 hrs)	[m]	-21.2	-45.5	-53.3	-50.8

Table 4 - Input data and results of the frequency-domain computations

Loaded tanker/Harris-DnV wind spectrum

Data		Wind spectrum V_w = 30.9 m/s	Wave spectrum	1-minute gust V_w = 36.5 m/s Wave spectrum	Wind spectrum V_w = 30.9 m/s Wave spectrum
INPUT DATA FOR FREQUENCY DOMAIN:					
a_{11}	[tf.s^2.m]	1594.0	1594.0	1594.0	1594.0
m	[tf.s^2.m]	24553.0	24553.0	24553.0	24553.0
b_{11}	[tf.s.m^{-1}]	17.9	17.9	17.9	17.9
b_{1v}	[tf.s.m^{-1}]	5.8	0.0	6.9	5.8
B_{11}	[tf.s.m^{-1}]	0.0	34.3	34.3	34.3
b(tot)		23.7	52.2	59.1	58.0
c_{11}	[tf.m^{-1}]	13.9	13.9	13.9	13.9
$x_1^{(2)}$	[tf]	0.0	-115.4	-115.4	-115.4
$x_{1v}^{(1)}$	[tf]	-89.6	0.0	-125.2	-89.6
$x_{1v}^{(2)}$	[tf]	-0.5	0.0	0.0	-0.5
X_1(tot)		-90.1	-115.4	-240.6	-205.5
$S_{x_1^{(2)}}$	[tf^2.s]	0.0	79212.0	79212.0	79212.0
$S_{x_{1v}^{(1)}}$	[tf^2.s]	1311.0	0.0	0.0	1311.0
$S_{x_{1v}^{(2)}}$	[tf^2.s]	9.0	0.0	0.0	9.0
S_{X_1}(tot)		1320.0	79212.0	79212.0	80532.0
FREQUENCY DOMAIN					
$\bar{x}_1$	[m]	-6.5	-8.3	-17.3	-14.8
σ_{x_1}	[m]	2.5	13.1	12.3	12.5
T_1	[s]	272.0	272.0	272.0	272.0
N (3 hrs)	[-]	39.7	39.7	39.7	39.7
x_{max} (3 hrs)	[m]	-13.3	-43.8	-50.7	-48.8

Table 5 - Input data and results of the frequency-domain computations

Ballasted tanker/Harris-DnV wind spectrum

Data		Wind spectrum V_w = 30.9 m/s	Wave spectrum	1-minute gust V_w = 36.5 m/s Wave spectrum	Wind spectrum V_w = 30.9 m/s Wave spectrum
INPUT DATA FOR FREQUENCY DOMAIN:					
a_{11}	$[tf.s^2.m]$	250.0	250.0	250.0	250.0
m	$[tf.s^2.m]$	9295.0	9295.0	9295.0	9295.0
b_{11}	$[tf.s.m^{-1}]$	16.0	16.0	16.0	16.0
b_{1w}	$[tf.s.m^{-1}]$	7.2	0.0	8.4	7.2
B_{11}	$[tf.s.m^{-1}]$	0.0	10.7	10.7	10.7
b(tot)		23.2	26.7	35.1	33.9
c_{11}	$[tf.m^{-1}]$	13.9	13.9	13.9	13.9
$X_1^{(2)}$	$[tf]$	0.0	-88.9	-88.9	-88.9
$X_{1w}^{(1)}$	$[tf]$	-110.4	0.0	-154.0	-110.4
$X_{1w}^{(2)}$	$[tf]$	-0.6	0.0	0.0	-0.6
$X_1(tot)$		-111.0	-88.9	-242.9	-199.9
$S_{X_1^{(2)}}$	$[tf^2.s]$	0.0	43260.0	43260.0	43260.0
$S_{X_1^{(1)}}$	$[tf^2.s]$	1991.0	0.0	0.0	1991.0
$S_{X_{1w}^{(2)}}$	$[tf^2.s]$	14.0	0.0	0.0	14.0
$S_{X_1^{1w}(tot)}$		2005.0	43260.0	43260.0	45265.0
FREQUENCY DOMAIN					
$\bar{x}_1$	$[m]$	-8.0	-6.4	-17.5	-14.4
σ_{x_1}	$[m]$	3.1	13.5	11.8	12.3
T^{x_1}	$[s]$	165.0	165.0	165.0	165.0
N (3 hrs)	$[-]$	65.5	65.5	65.5	65.5
x_{max} (3 hrs)	$[m]$	-17.0	-45.5	-51.6	-49.9

Table 6a - Input data and results of the frequency-domain computations

Loaded tanker/"2π-enhanced" Ochi-Shin vind spectrum

Data	Wind spectrum $V_w = 30.9$ m/s	Wave spectrum	1-minute gust $V_w = 39.7$ m/s Wave spectrum	Wind spectrum $V_w = 30.9$ m/s Wave spectrum
INPUT DATA FOR FREQUENCY DOMAIN:				
a_{11} [tf.s².m]	1594.0	1594.0	1594.0	1594.0
m [tf.s².m]	24553.0	24553.0	24553.0	24553.0
b_{11} [tf.s.m⁻¹]	17.9	17.9	17.9	17.9
b_{1v} [tf.s.m⁻¹]	5.8	0.0	7.5	5.8
B_{11} [tf.s.m⁻¹]	0.0	34.3	34.3	34.3
$b(tot)$	23.7	52.2	59.7	58.0
c_{11} [tf.m⁻¹]	13.9	13.9	13.9	13.9
$x_1^{(2)}$ [tf]	0.0	-115.4	-115.4	-115.4
$x_{1v}^{(1)}$ [tf]	-89.6	0.0	-147.9	-89.6
$x_{1v}^{(2)}$ [tf]	-5.7	0.0	0.0	-5.7
$X_1(tot)$	-95.3	-115.4	-263.3	-210.7
$S_{x_1^{(2)}}$ [tf².s]	0.0	79212.0	79212.0	79212.0
$S_{x_1^{(1)}}$ [tf².s]	17455.0	0.0	0.0	17455.0
$S_{x_{1v}^{(2)}}$ [tf².s]	1533.0	0.0	0.0	1533.0
$S_{x_1}(tot)$	18988.0	79212.0	79212.0	98200.0
FREQUENCY DOMAIN				
$\bar{x}_1$ [m]	-6.9	-8.3	-18.9	-15.2
σ_{x_1} [m]	9.5	13.1	12.2	13.8
T [s]	272.0	272.0	272.0	272.0
N (3 hrs) [-]	39.7	39.7	39.7	39.7
x_{max} (3 hrs) [m]	-32.7	-43.8	-52.0	-52.6

Table 6b - Results of the time-domain computations and model tests

Loaded tanker/"2π-enhanced" Ochi-Shin vind spectrum

Data	Wind spectrum $V_w = 30.9$ m/s	Wave spectrum	1-minute gust $V_w = 39.7$ m/s Wave spectrum	Wind spectrum $V_w = 30.9$ m/ Wave spectrum
TIME DOMAIN (duration 60 hrs)				
$\bar{x}_1$ [m]	-6.9	-8.4	-19.1	-15.3
σ_{x_1} [m]	9.2	13.4	12.6	13.9
T [s]	275.0	271.0	271.0	270.0
N (3 hrs) [-]	39.3	39.9	39.9	40.0
x_{max} (3 hrs) [m]	-32.9	-48.6	-56.7	-55.4
MODEL TESTS (duration 6 hrs)				
$\bar{x}_1$ [m]	-6.62	-7.8	-18.1	-13.5
σ_{x_1} [m]	11.95	12.5	12.5	13.9
T [s]	267.0	254.0	254.0	267.0
N (3 hrs) [-]	40.4	42.5	42.5	40.5
x_{max} (3 hrs) [m]	-33.0	-40.0	-52.0	-55.0
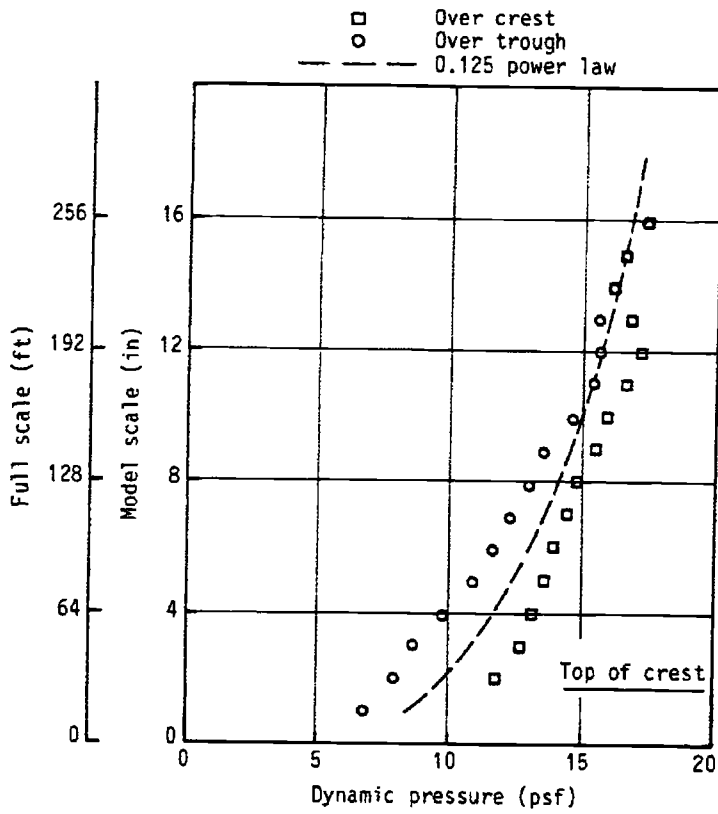
Fig. 1 - Vertical profiles of dynamic pressure of
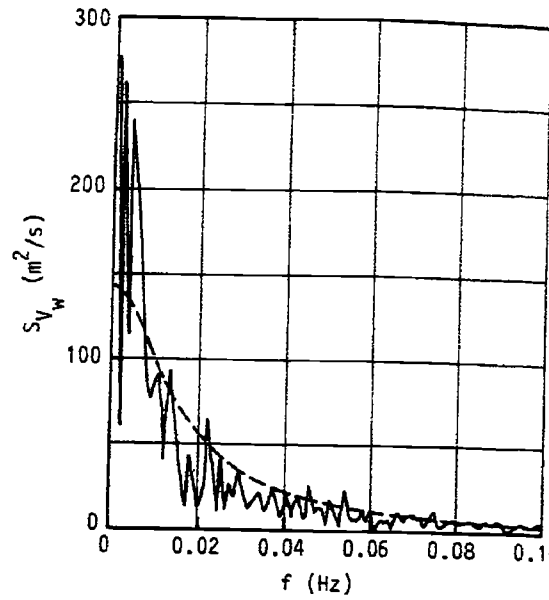wind measured over rigid wavy boundary

Fig. 2 - Wind spectrum measured from Eloi
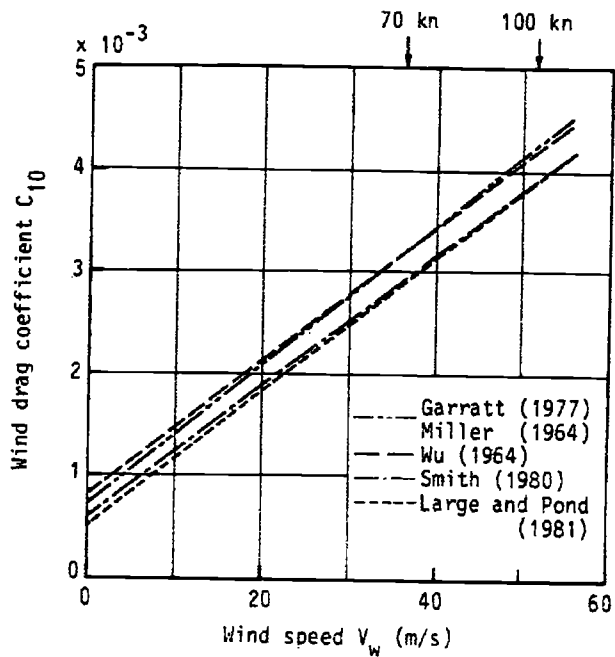at EI331 in comparison with DnV
spectrum formulation (ref. [3])

Fig. 3 - Wind drag coefficient as function of
mean wind speed V_w at the reference
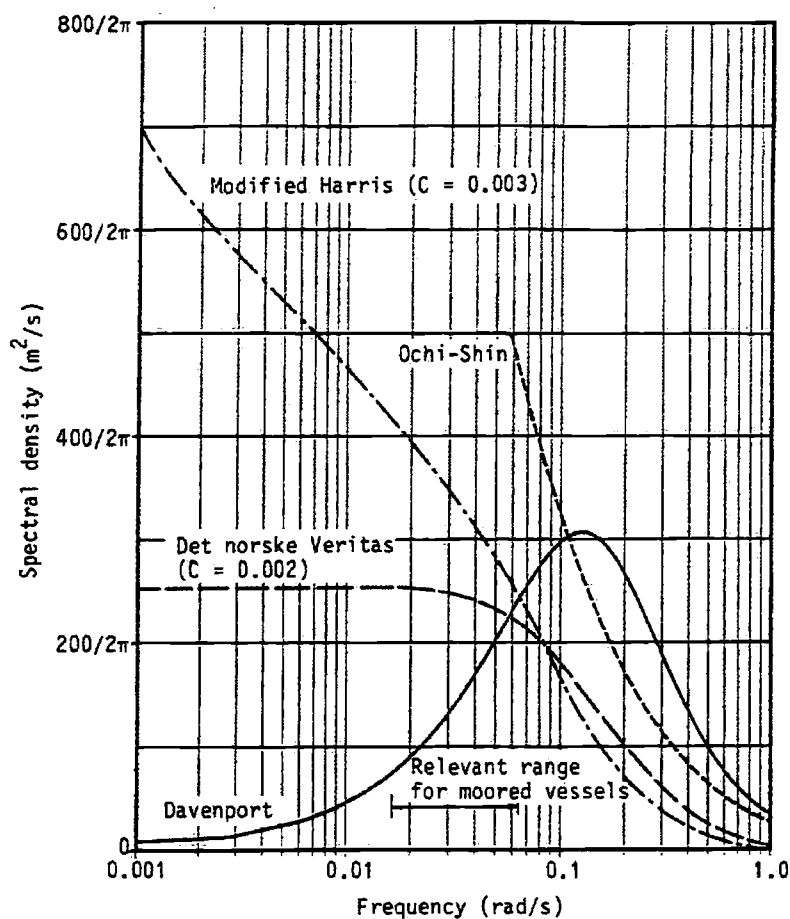level of 10 m (ref. [5])

Fig. 4 - Spectral densities following the formulation of Harris-DnV, Davenport, Ochi-Shin and Wills wind spectra (V_w = 30.9 m/s)
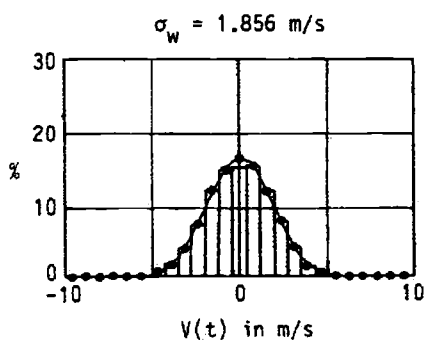

Fig. 5 - Distribution of instantaneous values of wind velocity (ref. [9])
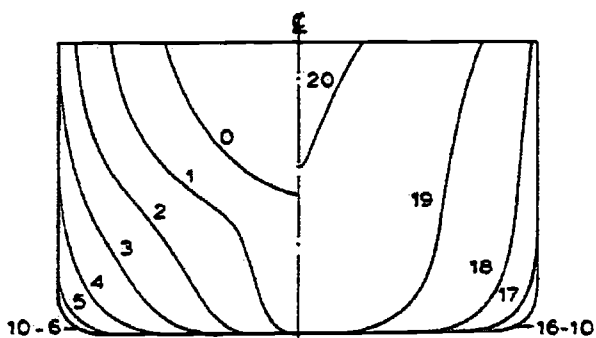
Fig. 6 - Body plan of the 200 kDWT tanker

Spring components (tf/m)						Resulting spring C_{xx} (tf/m)^{xx}
C_1	C_2	C_3	C_4	C_5	C_6	
14.0	14.0	14.1	14.1	4.6	4.6	13.9
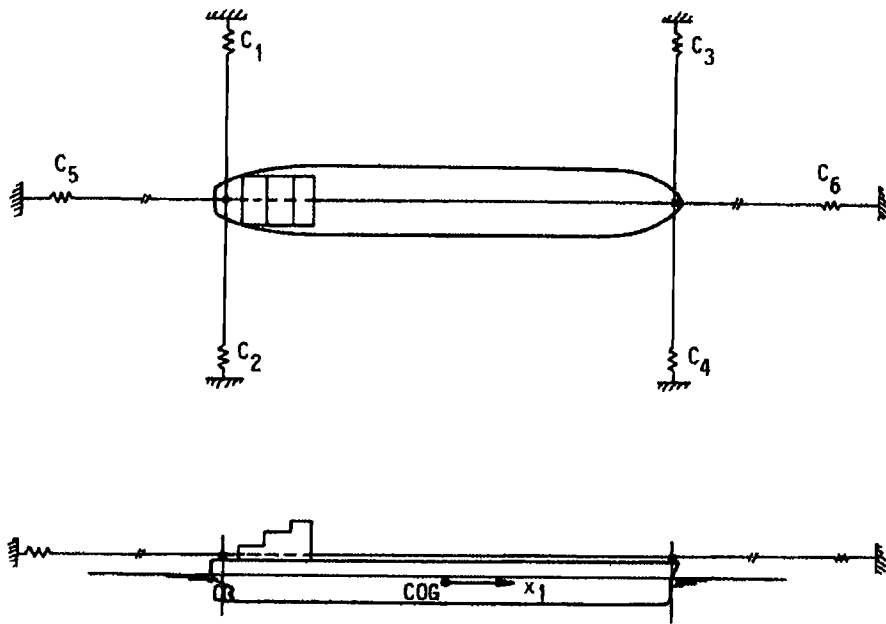
Fig. 7 - Set-up of the linearly moored tanker
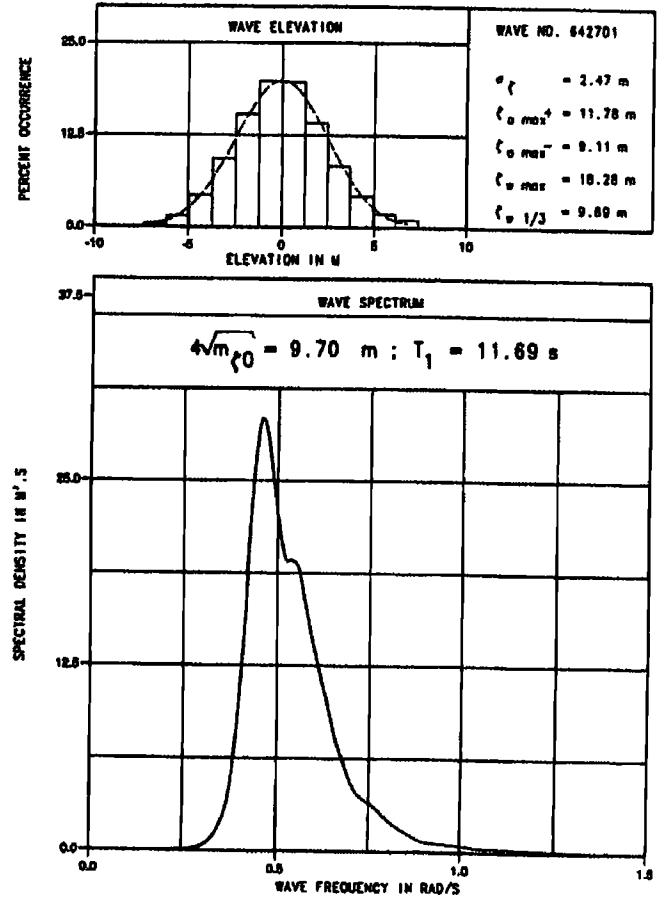
Fig. 8 - Wave spectrum
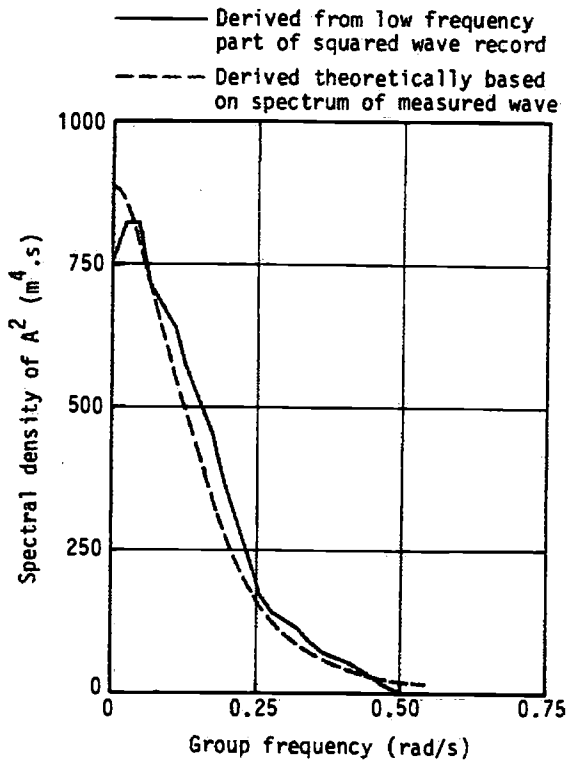
Fig. 9 - Wave group spectrum
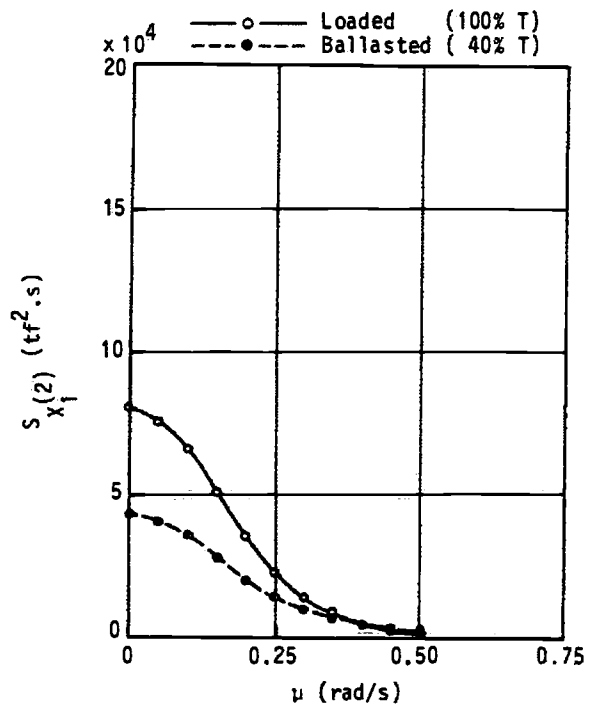
Fig. 10 - Wave drift force spectrum
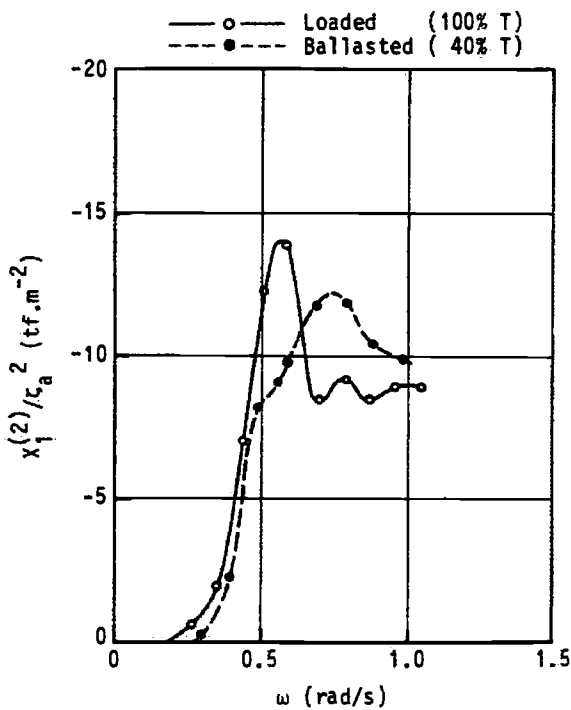
Fig. 11 - Quadratic transfer function of the wave drift force in longitudinal direction
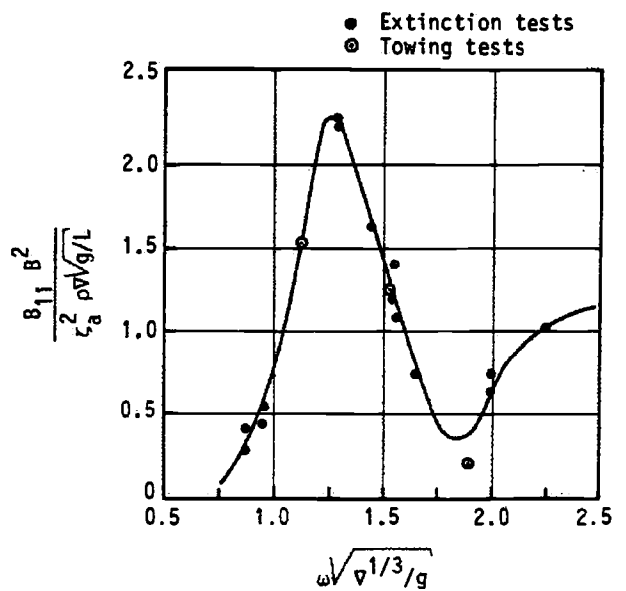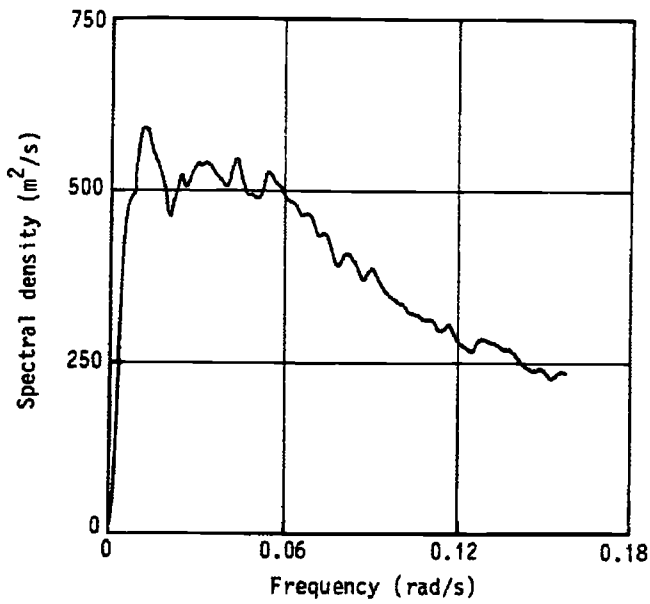

Fig. 12 - Wave drift damping quadratic transfer function

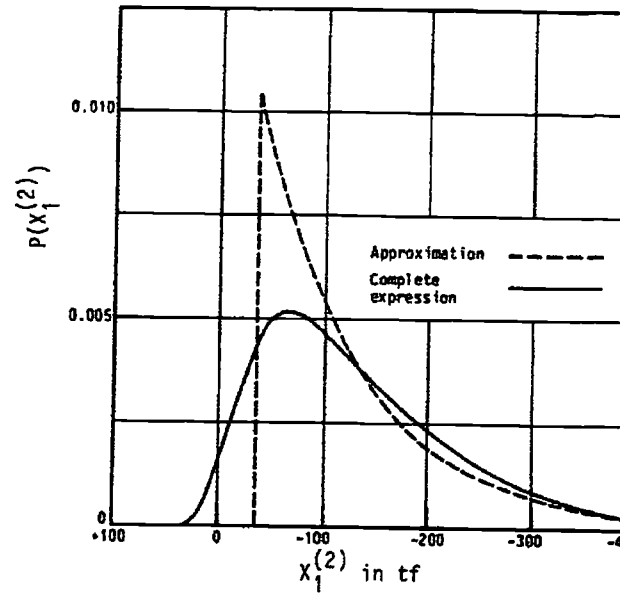Fig. 13 - Generated 2π-enhanced wind spectrum for
computations

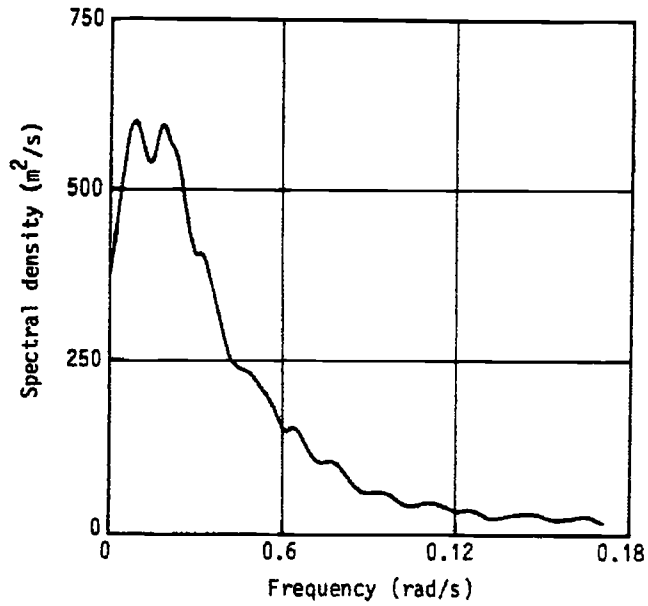Fig. 14 - Distribution of the wave drift forces
(ref. [13])

Fig. 15 - Generated 2π-enhanced wind spectrum in
the basin